Electronic Supplementary Material (ESI) for RSC Advances.

High-Throughput Microfluidic Platform for Adherent Single Cells Non-Viral Gene Delivery

Paola Occhetta,[a] Chiara Malloggi,[b] Andrea Gazaneo,[a] Alberto Redaelli,[a] Gabriele Candiani,[bcd] Marco Rasponi[a*]

Supplementary information

Computational optimization of the chamber geometry for single cell trapping

The design of the chamber element was optimized for single cell trapping by means of Computational Fluid Dynamic modeling (CFD, Comsol Multiphysics). The geometry considered for the analysis consisted in three chambers, provided with traps and connected through a bending main channel. As reported in Table SI1, eight possible geometrical configurations were considered, as combinations of four different widths of the fluidic channels (25, 50, 75 and 100μm) and two widths of the trapping elements (10 and 15μm). The heights of fluidic and trapping layers were fixed at 25μm and 5μm, respectively. Trapping junctions were modeled with rounded shaped cross-sections, with the aim of minimizing the trapping effective area, while matching fabrication requirements. The geometries were discretized through a tethraedrical mesh scheme, consisting of about $450x10^3$ and $670x10^3$ elements, for occluded and open configurations, respectively. The flow field was computed by solving stationary Navier–Stokes equations for incompressible fluids, setting the density and the viscosity equal to those of water at 25°C (1000 kg/m^3 and 0.890 cP, respectively). A uniform velocity profile was applied to the inlet, corresponding to a total inflow of 0.2μL/min, while a zero pressure condition was set to the outlet. A no-slip condition was applied to boundary walls. Convergence criterion was satisfied when the normalized residuals for the velocities fell below 1×10^{-6}.

Table SI1. Chamber layouts analyzed by means of CFD model. The layouts differ for both the channel and the trap width, while maintaining constant the channel and the trap height at 25μm and 5μm, respectively.

Chamber Layout	Channel width [μm]	Trap width [μm]
1	25	10
2	25	15
3	50	10
4	50	15
5	75	10
6	75	15
7	100	10
8	100	15

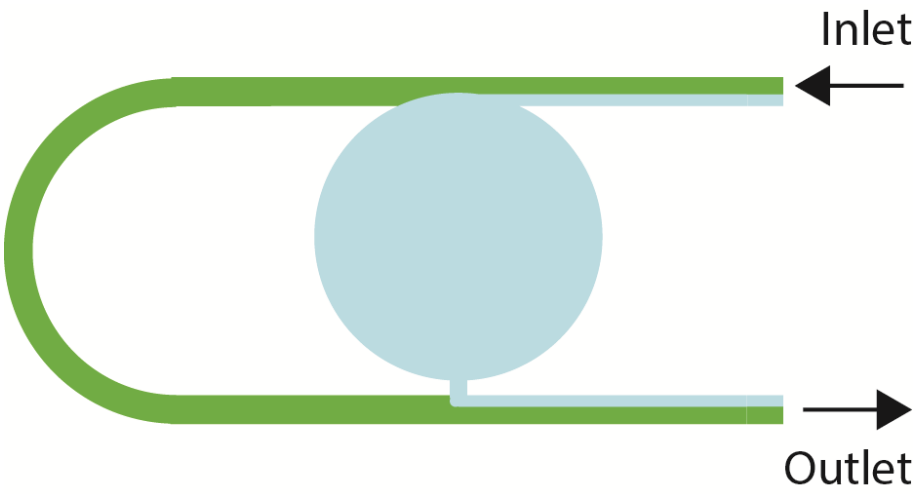

Fig. SI1 *Schematic representation of the partition of the circulating flow in the proximity of a chamber opening. The total fluid flow splits into two different fluidic paths, one entering the chamber (light blue lane) and the other still flowing in the main channel (green lane). The portion of the flow entering the chamber (Q_{in}) depends both on the main channel geometry and on the percentage of occlusion of the trapping junction.*

The inflow entering each chamber was assessed in both open and occluded configurations. In details, a schematic representation of the flow partition within a trapping chamber is shown in Fig.SI1. At each flow rate, the portion of the flow entering the chamber (Q_{in}), depicted as a light blue lane in Fig.SI1, depends both on the main channel geometry and on the percentage of occlusion of the trapping junction. The main channel can thus be divided in two distinct lanes, one entering the chamber (and having a width roughly proportional to Q_{in}) and the other bypassing it. In typical microfluidic flows, round suspended particles (i.e. cells) tend to follow the streamline ideally passing through their center of mass (CM). However, particle's CM cannot approach walls to a distance shorter than the particle radius, thus the minimum Q_{in} required to bring cells into a chamber corresponds to an entering lane (light blue, Fig.SI1) as wide as the particle's radius (Q_{lim}).

Ideally, the more Q_{in} is above Q_{lim} the higher are the occurrences of cells entering the chambers (and eventually being trapped), and viceversa. As a consequence, for a geometrical configuration to properly trap single cells, the following conditions must apply: $Q_{in} > Q_{lim}$ in open configuration, and $Q_{in} < Q_{lim}$ in the occluded configuration.

Q_{lim} values were numerically estimated and compared to Q_{in} (Fig.SI2a). For all the considered combinations of channels and traps, Q_{in} resulted higher than Q_{lim}, thus indicating all configurations as compatible with the trapping of cells in the selected size range (Φ=10-16μm). Regarding the occluded configuration, different results were obtained based on the diameter of simulated trapped cells. For bigger cells (Φ=16μm) Q_{in} resulted smaller than Q_{lim} for all combinations, indicating their ability to trap single cells. For smaller cells (Φ=10μm), only the small trap configuration was able to catch single cells, while occluded large traps failed to reduce the inflow below Q_{lim} thus being

unsuitable to isolate single cells. Indeed, despite the height of the trapping junction (5µm) is small enough to physically block a cell, its relatively large width (15µm) does not allow a sufficient occlusion when smaller cells are considered. As a consequence, 10µm wide traps resulted more effective in trapping single cells over a broader range of cell sizes, and this trap dimension was chosen for following analyses.

In order to identify the width of the main channel, an index of robustness, named selectivity index (SI), was further defined as the percentage difference between Q_{lim} and Q_{in} in each occluded configuration:

$$SI = 100 * \frac{(Qlim - Q_{in})}{Qlim}$$

Larger SI indexes indicate higher probability to inhibit cell entrance in a chamber where a cell is already blocking its trap. SI indexes were evaluated considering occlusions with cells having a diameter of 10µm. As shown in Fig.SI2b, the 50µm wide channel maximized trap selectiviy, yielding the highest probability to only trap single cells.

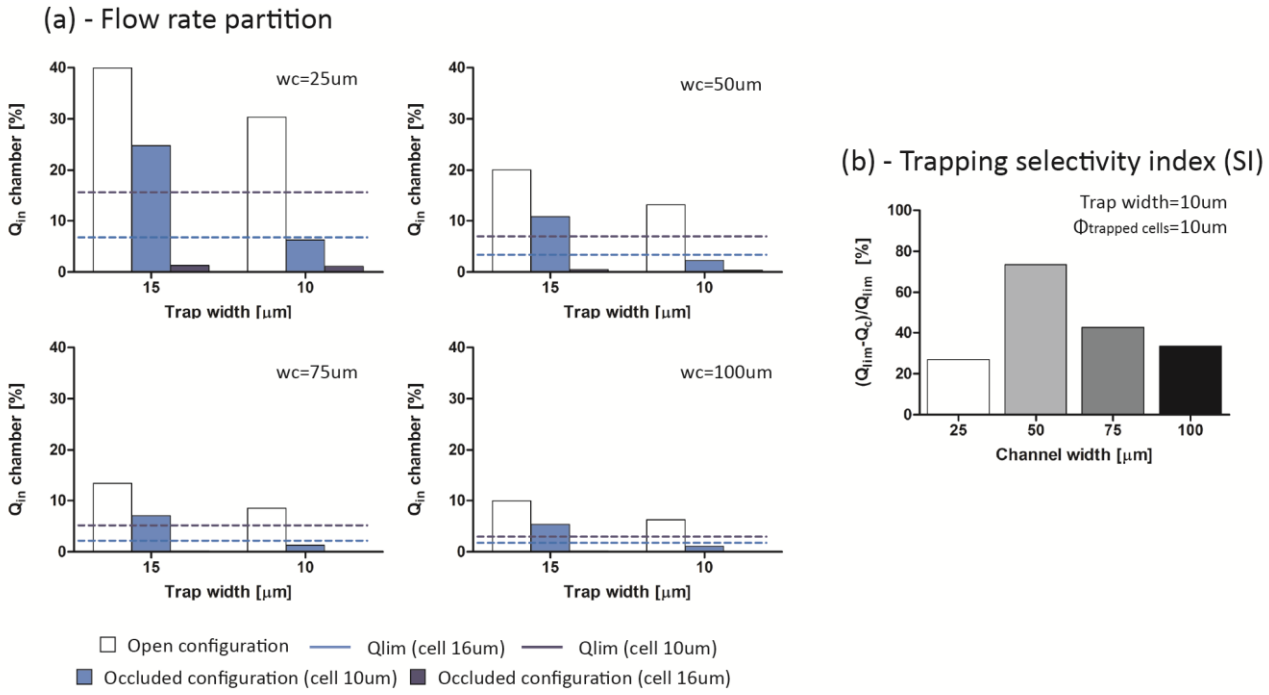

Fig. SI2 *Distribution of the flow rate inside chamber in open and closed configurations (for both 10µm and 16µm trapped cells) for the eight considered layouts. The results were then compared with Qlim (a) Trapping selectivity index trend for the layouts featuring 10µm wide traps considering trapped cells with a diameter of 10µm (b).*

Computational optimization of the chaotic mixer serial dilution generator

A serial dilution generator (SDG) element provided with chaotic enhanced mixing features was optimized by means of CFD analysis for mixing both soluble factors (*i.e.* growth factors) and non-diffusive assemblies (*i.e.* polyplexes), splitting an initial concentrated solution into 6 linear dilutions (from 0% to 100% in steps of 20%). In details, a T junction was designed to merge two different fluids, and a series of straight mixing elements were added downstream. The mixing elements were either repeating HB units (each unit 416μm long) or rectangular cross-sectional channels as controls. The geometries were discretized with a tethraedrical mesh scheme, consisting of about 195×10^3 and 20×10^3 elements, in the case of the presence and absence of HB, respectively. The flow field was computed by solving stationary Navier–Stokes equations for incompressible flow, setting the density and the viscosity equal to those of water at 25°C (1000 kg/m^3 and 0.890 cP, respectively). Uniform velocity profiles were applied to the inlets, corresponding to Reynolds numbers (Re) comprised between 0.1 and 10 (Q=0.255-25.5μL/min), while a zero pressure condition was set to the outlet. A no-slip condition was applied to the boundary walls. Convergence criterion was satisfied when the normalized residuals for the velocities fell below 1×10^{-6}. The injection of two differently concentrated non-diffusive species was performed into the inlets, and the profiles of concentration in all output channels were computed by means of the Transport of Diluted Species application module.

Fig.SI3 shows the trend of concentrations for Re=0.1, demonstrating the achievement of a complete mixing of species through the repetition of only ten HBs units (total length=4.2mm) (a), while no significant mixing was detectable in a rectangular channel featuring the same total length (b). The addition of HB grooves thus demonstrated to enhance the mixing of non-diffusive entities and, in the same time, require a lesser occupation of footprint in the device area.

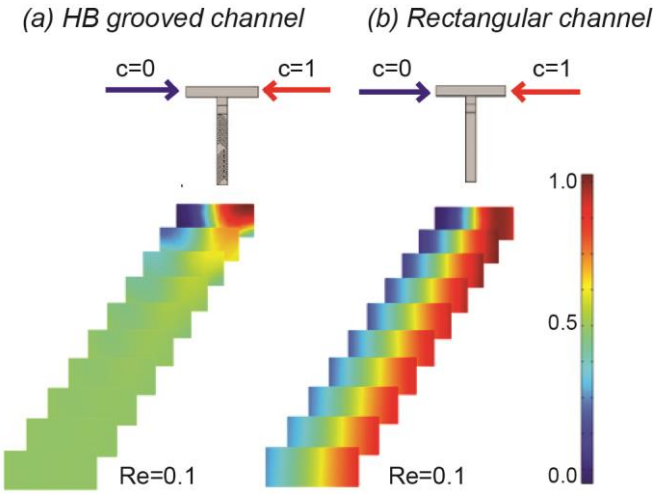

Fig.SI3 *Staggered herringbone (HB) grooves were integrated on the top of the SDG channels for enhancing the mixing of non-diffusive entities. CFD simulations were computed to verify the mixing efficacy of such structures (a) in comparison with rectangular channels (b). A complete mixing between two differently concentrated non-diffusive species was achieved flowing through a 4.2mm long HB grooved channel (a), while no mixing is observed for a rectangular channel featuring the same length (b). Showed results were obtained for Re=0.1.*

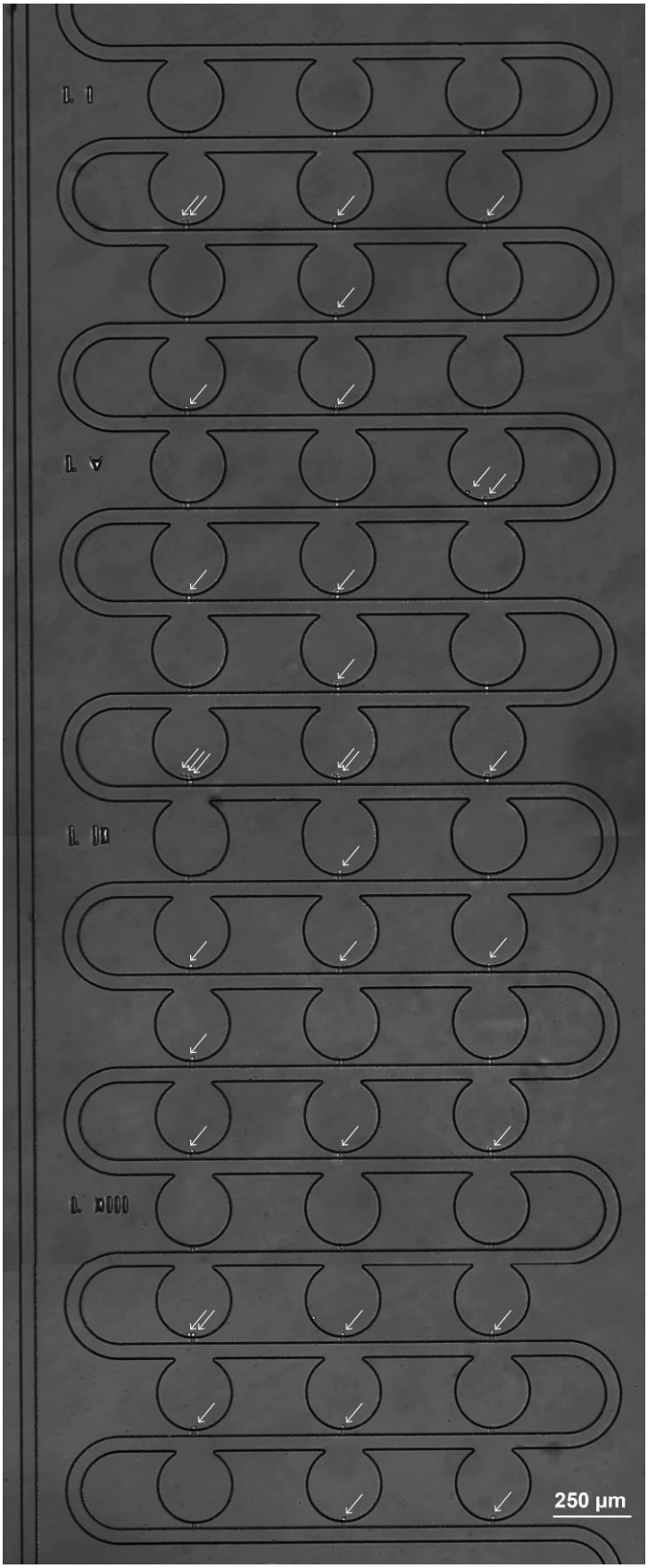

Fig. SI4 *Single cells trapped within a culture unit of the microfluidic platform. An average single cell trapping efficiency of 39.8±6.2 % was estimated.*

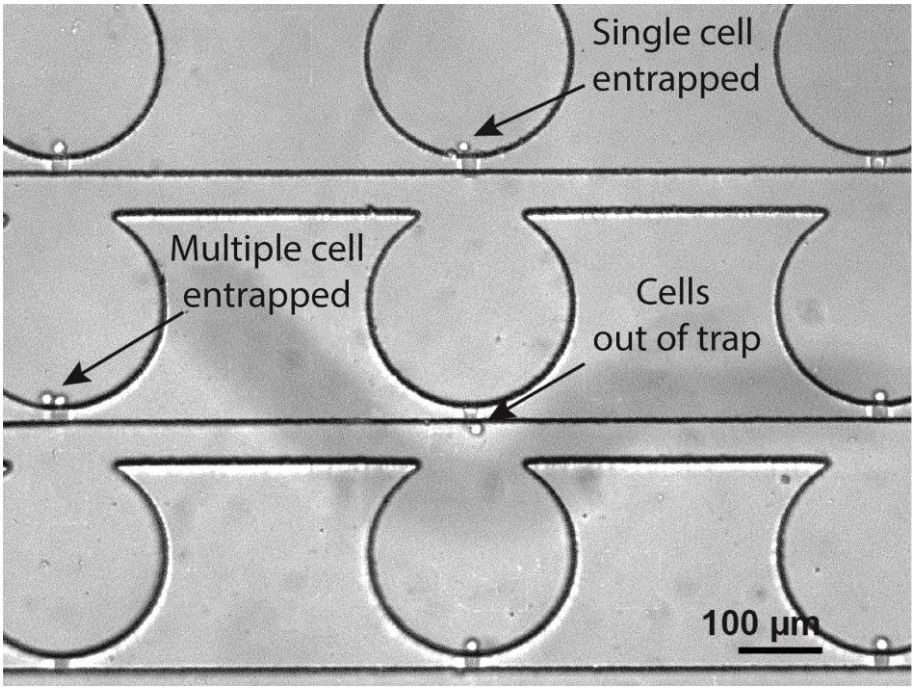

Fig. SI5 *The percentage of filled chambers after the seeding was calculated as the sum of three different possible occurrences, all depicted in this picture: 1) a single cell blocked within the trap; 2) multiple cells blocked within a trap; 3) the presence of cells out of the trap.*

–